Carbohydrate Polymers 121 (2015) 122–131

Contents lists available at ScienceDirect

Carbohydrate Polymers

journal homepage: www.elsevier.com/locate/carbpol

Polyelectrolyte nanocomplex formation of heparin-photosensitizer conjugate with polymeric scavenger for photodynamic therapy

Li Li [a], Hana Cho [b], Sungwon Kim [c], Han Chang Kang [b], Kang Moo Huh [a,*]

[a] Department of Polymer Science and Engineering, Chungnam National University, 99 Daehak-ro, Yuseong-gu, Daejeon 305-764, Republic of Korea
[b] Department of Pharmacy and Integrated Research Institute of Pharmaceutical Sciences, College of Pharmacy, The Catholic University of Korea, 43 Jibong-ro, Wonmi-gu, Bucheon-si, Gyeonggi-do 420-743, Republic of Korea
[c] R&D Center, LG Life Sciences, 188 Munji-ro, Yuseong-gu, Daejeon 305-738, Republic of Korea

ARTICLE INFO

Article history:
Received 14 October 2014
Received in revised form 3 December 2014
Accepted 3 December 2014
Available online 31 December 2014

Keywords:
Photodynamic therapy
Photosensitizer
Nanocomplex
Singlet oxygen
Scavenger
Polymer

ABSTRACT

A polyelectrolyte nanocomplex was prepared via the ionic interaction between the anionic heparin-pheophorbide a (HPhA) conjugate, which served as a water-soluble polysaccharide photosensitizer (PS), and the cationic polyethylenimine (PEI)-β-carotene (PCAR) conjugate, which served as a polymeric scavenger. This nanocomplex was designed to improve the water solubility and tumor specificity of PhA and to only release singlet oxygen at the tumor cell. A stable 150 nm-sized nanocomplex could be formed in the weight ratio range (PCAR/HPhA) of 0.3–0.5 in an aqueous environment. The PCAR scavenger significantly diminished the generation of active singlet oxygen from HPhA in a buffer solution. Singlet oxygen scavenging activity was lost only when HPhA and PCAR were separated from each other due to the dissociation of the complex nanostructures. It was confirmed that HPhA itself has neither colloidal properties nor a decrease in its ability to produce singlet oxygen. At the same time, the HPhA/PEI complex produced singlet oxygen in response to light. In a cell culture system, the cytotoxicity of the HPhA/PCAR nanocomplex toward cancer cells was greatly enhanced due to the efficient generation of singlet oxygen under light irradiation; this finding implies that the scavenging activity of PCAR can be restricted to intracellular environments. These results suggest that the HPhA/PCAR nanocomplex could provide a new activatable PS platform that facilitates more accurate and reliable photodynamic therapy (PDT) with site-specific and controllable production of singlet oxygen to be used for the treatment of cancer.

1. Introduction

Photodynamic therapy (PDT) has been widely applied in the clinic as a non-invasive therapeutic regimen to treat cancer (Dolmans, Fukumura, & Jain, 2003; Juarranz, Jaen, Sanz-Rodriguez, Cuevas, & Gonzalez, 2008; Wilson, 2002). In PDT, photosensitizing agents, or photosensitizers (PSs), are typically administered via intravenous routes; PSs are supposed to accumulate at tumor sites (Hamblin & Mróz, 2008; MacDonald & Dougherty, 2001). Upon light irradiation with a specific wavelength, PSs activate and generate highly reactive singlet oxygen from nearby oxygen molecules. This process results in tumor cell death and proximal tissue necrosis (Fernandez, Bilgin, & Grossweiner, 1997; Vrouenraets, Visser, Snow, & van Dongen, 2003). Most clinically available PSs (e.g., porphyrin and phthalocyanine derivatives) have drawbacks, such as poor water solubility and low tumor cell selectivity (Detty, Gibson, & Wagner, 2004; Konan, Gurny, & Allemann, 2002). The lack of tumor specificity often leads to unexpected damage to normal tissues; skin photosensitivity can also occur, even to some indoor light sources (Detty et al., 2004; Vrouenraets et al., 2003).

For successful PDT via PS delivery to tumor cells, the following two requirements should be fulfilled: the controllable generation of singlet oxygen and the tumor-selective accumulation of PSs (Li, Nurunnabi, Nafiujjaman, Jeong, Lee, & Huh, 2014; Li, Nurunnabi, Nafiujjaman, Lee, & Huh, 2013; Lovell, Liu, Chen, & Zheng, 2010; Park, Park, & Na, 2011; Verhille et al., 2010). During PDT, photodamage to target cells is highly dependent on the level of singlet oxygen generation stimulated by light irradiation. By controlling the generation of singlet oxygen, the level of singlet oxygen in the bloodstream is minimized, and the availability of active singlet oxygen within tumor tissue is maximized. The use of activatable PSs can satisfy this first requirement. Generally, activatable PSs generate singlet oxygen only within tumor tissues and remain inert during systemic circulation. For example, activatable PSs for targeted PDT can be constructed by the chemical conjugation of PS molecules

* Corresponding author. Tel.: +82 42 821 6663; fax: +82 42 821 8910.
E-mail address: khuh@cnu.ac.kr (K.M. Huh).

http://dx.doi.org/10.1016/j.carbpol.2014.12.035
0144-8617/

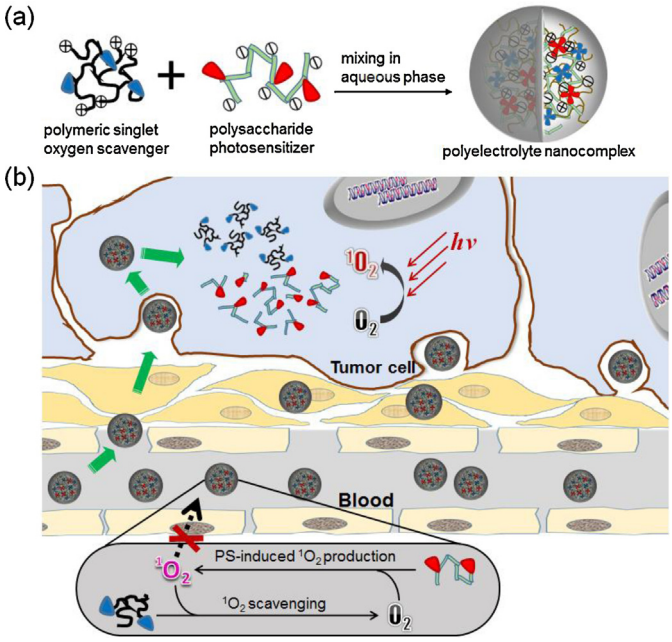

Fig. 1. Schematic concept of a proposed polyelectrolyte nanocomplex with tumor accumulation capacity via the enhanced permeability and retention effect (EPR) and the controllable production of singlet oxygen. (a) The nanocomplex designs to be prepared by ionic interactions between an anionic polysaccharide PS and a polymeric singlet oxygen scavenger. (b) The nanocomplexes do not produce cytotoxic reactive oxygen species during blood circulation because the polymeric scavenger depletes the generated singlet oxygen; therefore, the proposed nanocomplex is non-phototoxic during blood circulation and reduces the side effects observed with conventional PDT. When the nanocomplexes are internalized by cancer cells, the enzymatic degradation of polysaccharide chains and ionic exchange interactions induced by intracellular ions trigger the dissociation of the nanocomplexes. The PS and scavenger become spatially isolated, thereby restricting the scavenging effects and restoring the phototoxicity of the PS.

to a certain type of activation controller via stimuli-sensitive or cleavable linkers. Such linkers can be cleaved or degraded by physicochemical or biological stimuli that are specific to or over-expressed only within tumor tissue.

To date, activatable PSs have been constructed as low-molecular-weight systems such as PS–PS conjugates (McCarthy & Weissleder, 2007), PS-quencher conjugates (Lovell et al., 2009) or PS-singlet oxygen scavenger conjugates (Chen et al., 2007). Low-molecular-weight systems have limitations, such as the rapid elimination of conjugates from the body and the development of multiple drug resistance; these issues can result in short plasma half-life and low bioavailability (Master, Livingston, & Sen Gupta, 2013). Furthermore, the preparation of an activatable PS system often involves multiple synthetic procedures and purification steps. This poses a practical challenge to their application (Verhille et al., 2010).

Before the switching-on mechanism of the activatable PS in this study is presented, its physical structure and the theory of tumor targeting should be explained. We designed a polyelectrolyte nanocomplex platform produced by the ionic interaction between a water-soluble polysaccharide PS and a polymeric scavenger (Fig. 1(a)). Unlike conventional low-molecular-weight activatable PSs, the nanocomplex system is expected to have a prolonged blood circulation time due to its nanometer size and biocompatible particle surface. An increase in the selective accumulation of PSs at tumor sites is expected as a consequence of the enhanced permeability and retention (EPR) effect (Maeda, 2001; Nehoff, Parayath, Domanovitch, Taurin, & Greish, 2014); such accumulation is required for successful PDT. As shown in Fig. 1(b), the nanocomplex PS system has the potential to positively modulate pharmacokinetic and toxicological properties and the pharmacodynamic end-point of loaded PSs (Park et al., 2011).

In this study, an anionic heparin-pheophorbide a (HPhA) conjugate was synthesized as a water-soluble polysaccharide PS, and a cationic polyethylenimine (PEI)-β-carotene conjugate (PCAR) was synthesized as a polymeric scavenger. These components were utilized to produce nanocomplex PSs by the electrostatic interaction between oppositely charged polyelectrolytes. PhA has very low solubility in water; therefore, its practical utilization as a pharmaceutical agent has been limited (Robert, 1986). To overcome this problem, we synthesized a water-soluble PhA by conjugating it to heparin. Heparin, a negatively charged polysaccharide, has been used in the pharmaceutical and biomedical fields due to its excellent water solubility, biocompatibility, and biodegradability (Linhardt, 1991). CAR, a singlet oxygen scavenger, was introduced to control the availability of singlet oxygen generated from HPhA molecules. However, CAR is a small, hydrophobic molecule. It is therefore difficult to directly combine CAR with water-soluble HPhA conjugates. We conjugated CAR molecules to water-soluble branched PEI (bPEI) to create a positively charged macromolecular scavenger to be electrostatically complexed with HPhA. One advantage of the proposed nanocomplex over conventional activatable PSs is that the water-soluble form of this colloid-stable, nanometer-sized PS can be simply prepared by mixing two aqueous solutions of HPhA and PCAR without the use of an organic solvent or a complicated preparation process.

The HPhA/PCAR nanocomplex has tumor-site specificity and is easily prepared; in addition, it is designed to exhibit switchable phototoxicity. We previously described a PhA/CAR dual-loaded micellar system in which singlet oxygen production for PDT can be controlled (Li, Cho, Yoon, Kang, & Huh, 2014). In micelles, the antioxidant agent CAR significantly diminished singlet oxygen quantity through direct scavenging. Thus, the HPhA/PCAR nanocomplex is expected to restrict the phototoxicity of PhA and minimize the complications observed in traditional PDT. It is hypothesized that the intravenously administered nanocomplex is localized to tumor tissue and endocytosed by tumor cells. After internalization, HPhA and PCAR might dissociate via ionic exchange; heparin may also be degraded enzymatically. We predict that the spatial separation of PhA and CAR within cells can prevent the CAR-mediated scavenging of the singlet oxygen generated by the PhA, resulting in the switching-on of photodynamic therapy.

As a proof-of-principle study, this work aims at establishing the preparation conditions for the formation of an HPhA/PCAR nanocomplex with appropriate particle size and stability in a physiological environment. This nanocomplex was investigated with regard to its physicochemical characteristics, photoactivity, and in vitro PDT efficacy in tumor cell culture systems.

2. Materials and methods

2.1. Materials

Unfractionated heparin (MW 12,000 Da) was obtained from Mediplex Co. (Korea). Pheophorbide a (PhA) was purchased from Frontier Scientific Inc. (Logan, UT, USA). Branched polyethylenimine (bPEI) (MW 25,000 Da) was obtained from Sigma–Aldrich (St. Louis, MO, USA). *N*-(3-Dimethylaminopropyl)-*N*′-ethylcarbodiimide hydrochloride (EDC·HCl), trans-β-apo-8′-carotenal, sodium triacetoxyborohydride (STAB), 1,2-dichloroethane (DCE), acetic acid (AcOH), dimethyl sulfoxide (DMSO), 9,10-dimethylanthracene (DMA), 3-(4,5-dimethylthiazol-2-yl)-2,5-diphenyltetrazolium bromide (MTT), RPMI 1640 medium, Ca^{2+}- and Mg^{2+}-free Dulbecco's

phosphate-buffered saline (DPBS), 4-(2-hydroxy-ethyl)-1-piperazine (HEPES), D-glucose, sodium bicarbonate, glutathione monoethyl ester (GSHOEt), recombinant human insulin, fetal bovine serum (FBS), bovine serum albumin (BSA), and trypsin–EDTA solution were purchased from Sigma–Aldrich (St. Louis, MO, USA). Spectra/Por® membranes (Regenerated Cellulose, MWCO = 8000 Da) were purchased from Spectrum Laboratories, Inc. (Rancho Dominguez, CA, USA). All chemicals for polymer synthesis were at least analytical grade and were used without further purification.

2.2. Synthesis of anionic HPhA conjugates

Aminated PhA was synthesized as described in our previous report (Li et al., 2011) and conjugated to a heparin backbone through a coupling reaction between the amino group of animated PhA and the carboxyl group of heparin. Briefly, heparin (150 mg, 100 μmol carboxylic acids) and aminated PhA (40 mg, 66.7 μmol) were dissolved in formamide (5 mL) and DMF (5 mL), respectively. EDC·HCl (38.3 mg, 200 μmol) was added to the heparin solution. The heparin solution was then mixed with the PhA solution. The reaction was performed at room temperature under atmospheric nitrogen for 36 h. After the coupling reaction, the solution was dialyzed for 2 days. The solution was then filtered through a 0.2-μm syringe filter. The crude product was obtained after freeze-drying and washed with methanol to remove uncoupled PhA. The final HPhA product was collected by centrifugation and dried under vacuum. The coupling ratio for PhA was characterized using the colorimetric method described in our previous study (Li et al., 2011).

2.3. Synthesis of cationic PCAR conjugates

To prepare the PCAR conjugate, a CAR derivative, trans-β-apo-8′-carotenal, was conjugated to bPEI via reductive amination chemistry mediated by STAB. bPEI (625 mg, 25 μmol) and trans-β-apo-8′-carotenal (52 mg, 125 μmol) were mixed in DCE; the mixture was then treated with STAB (43 mg, 200 μmol) and AcOH (10 mg, 167 μmol). The mixture was stirred at room temperature under atmospheric nitrogen for 24 h. The resultant solution was precipitated in cold diethyl ether and dried in vacuo. The crude product was washed three times with acetone to remove unreacted trans-β-apo-8′-carotenal. The PCA conjugate was obtained by drying the product under vacuum. The chemical structure of PCAR was confirmed via ^{1}H NMR (JNM-AL 400 spectrometer, 400 MHz, JEOL Ltd., Tokyo, Japan). The content of the CAR conjugated to bPEI was measured using a colorimetric method. Briefly, in order to prepare the calibration curve for CAR, the free CAR was dissolved in 10 mL of DMF at various concentrations. The absorbance at 460 nm was determined using a UV-Visible spectrometer (SINCO PDA, UV/Visible spectrometer operation, Seoul, Korea). The CAR content in the PCAR conjugate was calculated based on a calibration curve for CAR (460 nm) in DMF (Fig. S1).

2.4. Preparation and characterization of the HPhA/PCAR nanocomplex

A series of PCAR solutions at various concentrations (0.4–1.2 mg/mL) and multiple HPhA solutions at a concentration of 2 mg/mL were prepared by dissolving the dry polymer powders in PBS (0.1 M, pH 7.4). The HPhA/PCAR nanocomplex was prepared by adding 2 mL of each PCAR solution to an equal volume of the HPhA solution in a glass vial under gentle stirring. The mixtures were then incubated for 30 min at room temperature. The control sample, the HPhA/PEI nanocomplex (HPhA:PEI = 5:1, weight ratio), was prepared using the same protocol. The compositions of the prepared HPhA/PCAR nanocomplexes are listed in Table 1. Freshly prepared HPhA/PCAR nanocomplex solutions were used in each experiment.

The particle size, size distribution, and zeta-potential of the HPhA/PCAR nanocomplexes were measured using a dynamic light-scattering instrument (ELS-Z series, Otsuka Electronics, Osaka, Japan). To assess the colloidal stability of the HPhA/PCAR nanocomplexes in PBS, the complex solutions were incubated in a shaking bath (200 rpm) at 37 °C. The change in particle size was monitored over time. The morphology of the nanocomplex was observed by TEM (JEM-2100F, JEOL Ltd., Tokyo, Japan). To prepare the samples, the nanocomplex solutions were dropped onto carbon-coated copper grids. After 15 min, the excess polymer solution was removed with filter paper. The grid was dried for at least 24 h, and samples were observed without staining.

The absorption spectra of free PhA in PBS and formamide, of HPhA in PBS and formamide, and of HPhA/PCAR nanocomplexes in PBS were monitored using a UV-Visible spectrometer. The concentration of PhA in each sample solution was synchronized (2.5 μg PhA equivalent/mL). To estimate the fluorescence spectrometric states of PhA in the HPhA conjugate, the HPhA/PEI nanocomplex, and the HPhA/PCAR nanocomplex, each sample was dispersed in PBS at a PhA concentration of 5 μg/mL; fluorescence emission spectra were recorded at 600–750 nm using a fluorescence spectrophotometer (Cary Eclipse, Varian, Palo Alto, CA, USA) with an excitation wavelength of 405 nm.

The singlet oxygen generation by the HPhA conjugate, the HPhA/PEI nanocomplex, and the HPhA/PCAR nanocomplex was assessed based on the decreasing fluorescence intensity of DMA as a singlet oxygen trap (Li et al., 2011). The HPhA conjugate and nanocomplexes were prepared in PBS (5 μg/mL of PhA equivalent). A solution containing HPhA and PCAR in formamide, which represented a soluble conjugate mixture, was also prepared. Each sample solution was mixed with a DMA solution to reach a final concentration of 1.184×10^{-2} mM DMA. The mixtures were irradiated using a 670-nm laser source (LWRL-100 K, Beijing Laserwave Optoelectronic Tech. Co., Beijing, China) at a light intensity of 4.2 mW/cm^2. The fluorescence intensity of the DMA (which has an emission wavelength of 380–550 nm and an excitation wavelength of 360 nm) was monitored using a fluorescence spectrometer. The singlet oxygen quantum yield (SOQ) was calculated as follows:

$$\phi_\Delta = \frac{K_S}{K_R} \times \frac{A_R}{A_S} \times \mathrm{ref} \cdot \phi_\Delta$$

where A is the absorbance at 670 nm (the excitation wavelength), K is the gradient of the absorbance curve, and the subscripts S and R refer to the sample and reference, respectively. The SOQ (ϕ_Δ) of each sample was calculated based on the reference ϕ_Δ value (free PhA, 0.52) (Li et al., 2011).

2.5. In vitro phototoxicity of the HPhA/PCAR nanocomplex toward cancer cells

MCF-7 cells were cultured in RPMI 1640 supplemented with 10% FBS and D-glucose (2 g/L). Insulin (4 mg/L) was added to the culture medium to stimulate the cell cycle progression of MCF-7 cells. The cells were maintained and grown under humidified air containing 5% CO_2 at 37 °C.

To evaluate dark toxicity and phototoxicity, the cells were exposed to free PhA, HPhA conjugates, or HPhA/PCAR nanocomplexes. The cells (5000 cells/well) were seeded in a black 96-well plate with a clear bottom and incubated for 24 h. The cells were then treated with solutions of free PhA, HPhA conjugates, or HPhA/PCAR nanocomplexes at various concentrations. The culture medium was changed at 12 h post-treatment, and the cells were irradiated with light at 1.7 J/cm^2 (8.67 mW, 63 s) to induce phototoxicity. At 36 h post-treatment, MTT solution (0.5 mg/mL) was added to the

Table 1
Preparation of HPhA/PCAR nanocomplexes.

	HPhA/PCAR nanocomplex					
Weight ratio of PCAR/HPhA	0.2	0.3	0.4	0.5	0.6	0.7
Size (nm)	N.D.	146.2 ± 3.4	155.1 ± 1.8	149.8 ± 4.1	N.T.	N.T.
Polydispersity index	N.D.	0.18 ± 0.01	0.14 ± 0.01	0.17 ± 0.02	N.T.	N.T.
Zeta-potential (mV)	N.D.	−30.9 ± 3.3	−8.0 ± 1.2	2.4 ± 1.6	N.T.	N.T.

N.D., not detected; N.T., no test.

cells; the cells were then incubated for an additional 4 h. After the MTT-containing medium was removed, the formazan crystals produced by the live cells were dissolved in DMSO (100 μL/well). The absorbance of the resulting solution was measured at 570 nm.

3. Results and discussion

3.1. Preparation and characterization of HPhA/PCAR nanocomplex

To fabricate a polyelectrolyte HPhA/PCAR nanocomplex with controllable photoactivity, an anionic HPhA conjugate as a polysaccharide PS and a cationic PCAR conjugate as a polymeric scavenger were first synthesized (Fig. 2). The nanocomplex was then simply prepared by the electrostatic complexation of the HPhA conjugate and the PCAR conjugate in an aqueous environment.

The HPhA conjugate was synthesized through a simple one-step carbodiimide coupling reaction between the amino group of the aminated PhA and the carboxyl group of heparin. The chemical structure of HPhA was confirmed by ^{1}H NMR. The characteristic chemical shifts for HPhA conjugates corresponding to heparin (3.4, 3.7, and 4.2 ppm) and aminated PhA (1.2, 1.9, 2.1, 3.1, 3.2, and 3.3 ppm) were observed in the ^{1}H NMR spectrum of HPhA (Fig. 3(a)). Because no laser scattering profile was observed in the aqueous HPhA solutions during the DLS measurement, we confirmed that the HPhA conjugates prepared in this work did not exhibit supramolecular assembly behavior. One possible explanation is that, although the log *P* value of PhA is approximately 3.7, the degree of substitution may be too low to effectively induce and stabilize an intermolecular interaction. It was found that the coupling ratio of PhA per heparin molecule was 2.67; this was determined using the colorimetric method. In addition, the strong negative charge of the unfractionated heparin could produce a significant electrostatic repulsion force between HPhA chains and may prevent the self-aggregation of HPhA conjugates. Therefore, HPhA molecules are able to exist as water-soluble conjugates rather than as self-assembled nanoparticles in an aqueous medium.

PCAR was synthesized by chemical coupling CAR with bPEI via reductive amination chemistry. An ^{1}H NMR spectrum of the PCAR conjugate is depicted in Fig. 3(b). The resonances at 1.0–2.0 and at 6.1–6.7 ppm were ascribed to the CAR moieties. The resonances of the —CH_2— protons of the bPEI chains appeared at 2.2–2.9 ppm. As confirmed by UV measurement, the coupling ratio of CAR per bPEI polymer chain was 2.96. In addition to their polyelectrolyte nature, the PCAR conjugates also exhibited good water-solubility as estimated by DLS.

To prepare the HPhA/PCAR nanocomplex, anionic and cationic polymers were dissolved separately in 0.1 M PBS (pH 7.4). The oppositely charged polyelectrolytes could be spontaneously assembled; a simple mixing process formed a nanoparticulate structure driven by an electrostatic interaction (Fig. 4(a)). To determine the optimal polymer ratio for producing a stable nanocomplex, HPhA/PCAR complexes were prepared by varying the PCAR-to-HPhA weight ratio (0.2–0.7, Table 1). There were no nanostructured complexes detected in the HPhA/PCAR solution at a PCAR/HPhA weight ratio of 0.2. This result indicated that a lower fraction of PCAR could not provide an appropriate charge ratio to force an effective coacervation. Conversely, higher fractions of PCAR (PCAR/HPhA weight ratios ≥0.6) yielded nondispersive agglomerates when the anionic and cationic polymers were mixed. As shown in Table 1, the optimal PCAR/HPhA weight ratio for the formation of a stable HPhA/PCAR complex with narrow nanosize distribution was between 0.3 and 0.5. In this range, a dynamic change in zeta-potential was observed when the PCAR amount was varied (Fig. 4(b)). The zeta potential of the HPhA/PCAR complex was highly negative (∼−31 mV) at a weight ratio of 0.3; the net charge of the nanoparticle was determined by the negatively charged HPhA. As the fractions of positively charged PCAR increased, the zeta-potential of the nanocomplex moved to −8 mV and then to 2.4 mV; these results indicate that the negative net charge was gradually neutralized by supplementing with PCAR. The hydrodynamic size of nanocomplexes was approximately 150 nm, as measured by DLS. No change in particle size was observed when the weight ratio of PCAR/HPhA increased from 0.3 to 0.5. A representative TEM image and a size distribution plot of the HPhA/PCAR nanocomplex are shown in Fig. 5(d) and (e), respectively. The complex nanoparticles were nearly spherical in appearance with a narrow size distribution. The colloidal stability of the HPhA/PCAR nanocomplexes was investigated in PBS at 37 °C. As shown in Fig. 5(c), the average size of the nanocomplexes remained unchanged after 5 days in PBS. The excellent aqueous stability of the HPhA/PCAR nanocomplexes suggests that their colloidal integrity could be retained for a certain period of time, even in physiological conditions (e.g., blood). Therefore, the HPhA/PCAR nanocomplex could be an elegant carrier platform for the selective delivery of PS due to its appropriate size, surface properties, and physical stability. It is commonly accepted that positively charged nanoparticles are less biocompatible and exhibit greater nonspecific adsorption to tissue than negatively charged nanoparticles. In the HPhA/PCAR complex system, the balance between CAR units and PhA units should be considered to achieve a desired singlet oxygen scavenging effect. For these reasons, the HPhA/PCAR nanocomplex at a PCAR/HPhA weight ratio of 0.4 was chosen to estimate the spectrometric properties, the generation of singlet oxygen, and the in vitro phototoxicity of the designed nanocomplex. For further experiments, an 80 nm-sized HPhA/PEI nanocomplex sample that was further characterized in terms of fluorescence intensity and singlet oxygen generation was used as a control.

3.2. Spectrometric characteristics of the HPhA/PCAR nanocomplex

To verify the extent of solubility of PhA in the nanocomplexes, the UV–vis spectra of HPhA/PCAR nanocomplexes in PBS was measured and compared with those of a HPhA conjugate or free PhA in PBS or in formamide (Fig. 5(a)). The free PhA in formamide had a strong absorption at 667 nm, indicating that the molecule exists in a monomeric form in formamide (Eichwurzel, Stiel, & Roder, 2000). However, the Q-band absorption of free PhA in PBS shifted toward longer wavelengths (e.g., 683 nm) compared with that of free PhA in formamide. The intensity of the absorption of free PhA in PBS was also lower. Together, these findings indicate that free PhA exists in its aggregated state in water. The HPhA conjugates

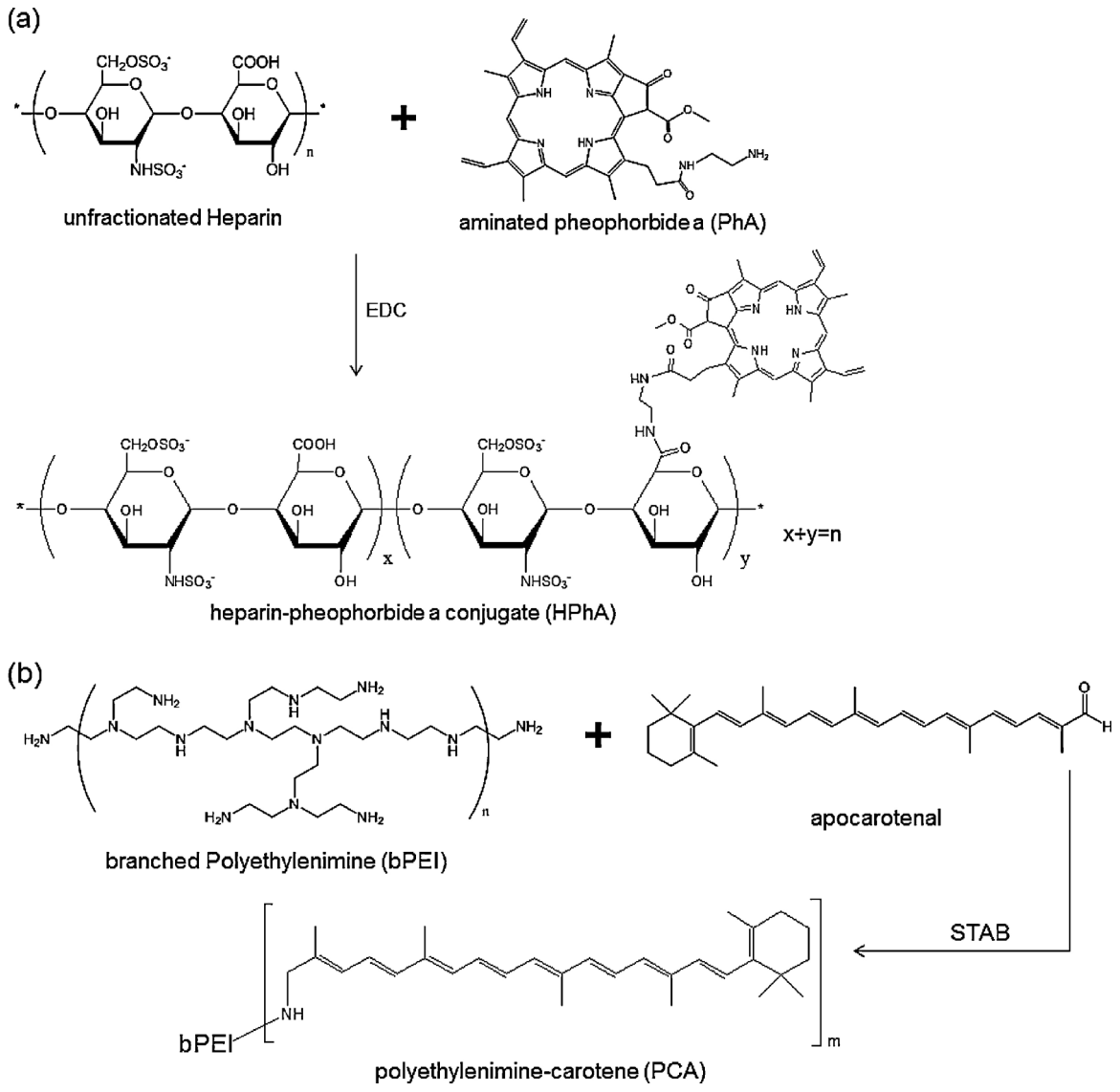

Fig. 2. Synthesis scheme for (a) the HPhA conjugate and (b) the PCAR conjugate.

in PBS had a Q-band absorption peak at 670 nm that was quite similar to that of free PhA in formamide at 667 nm; the Q-band intensity for the HPhA conjugates in PBS reached approximately 93% of the absorption intensity of free PhA in formamide, suggesting that conjugation with heparin chains creates a water-soluble form of PhA. The Q-band absorption peak for the nanocomplex appeared at 670 nm, and the intensity reached approximately 94% of the absorption intensity of free PhA in formamide. These readings are characteristic of the absorption of HPhA conjugates in PBS. This result indicates that the electrostatic complexation process did not result in the segregation or aggregation of PhA molecules in the nanocomplex. In addition, the characteristic absorption of PCAR at 455 nm appeared in the spectrum of the HPhA/PCAR nanocomplex. This implies that CAR co-exists in the nanocomplex. As a result, the HPhA/PCAR nanocomplex could preserve the spectrophotometric properties of PhA and CAR due to the enhanced aqueous solubility of both compounds aided by water-soluble polymers.

To assess the fluorescence spectrometric states of PhA in the HPhA/PCAR nanocomplex, the fluorescence emission spectrum of the HPhA/PCAR nanocomplex was monitored in PBS and compared with the spectra of free PhA, HPhA conjugates and the HPhA/PEI nanocomplex (as a negative control) in PBS. As shown in Fig. 5(b), free PhA produced a relatively low fluorescence intensity in PBS; this finding demonstrates that the compound exists in a photodynamically inactive state. Fluorescence resonance energy transfer (FRET)-based photoquenching was induced by the self-aggregation of PhA molecules via hydrophobic interactions and π–π stacking in an aqueous environment. HPhA conjugates in PBS, which presented as soluble polymer chains, exhibited an approximately 9-fold greater fluorescence intensity than that of free PhA. This suggests that the conjugated form of PhA inhibits the aggregation of PhA molecules in aqueous conditions, generating strong fluorescence. In addition, the PhA in HPhA/PEI and HPhA/PCAR nanocomplexes exhibited an approximately 4% and 8% lower fluorescence intensity, respectively, than the HPhA conjugates in PBS. These results imply that the complex formation and the presence of CAR scavengers have negligible effects on the spectrophotometric characteristics of PhA molecules. These findings corroborate the results in our previous report (Li, Cho, et al., 2014). The co-existence of CARs and PhAs that are physically entrapped in a system did not have a fluorescence quenching effect; however, molecules covalently bonded to CARs and PhA derivatives diminished the fluorescence of PhA molecules (Chen et al., 2007). Consequently, we

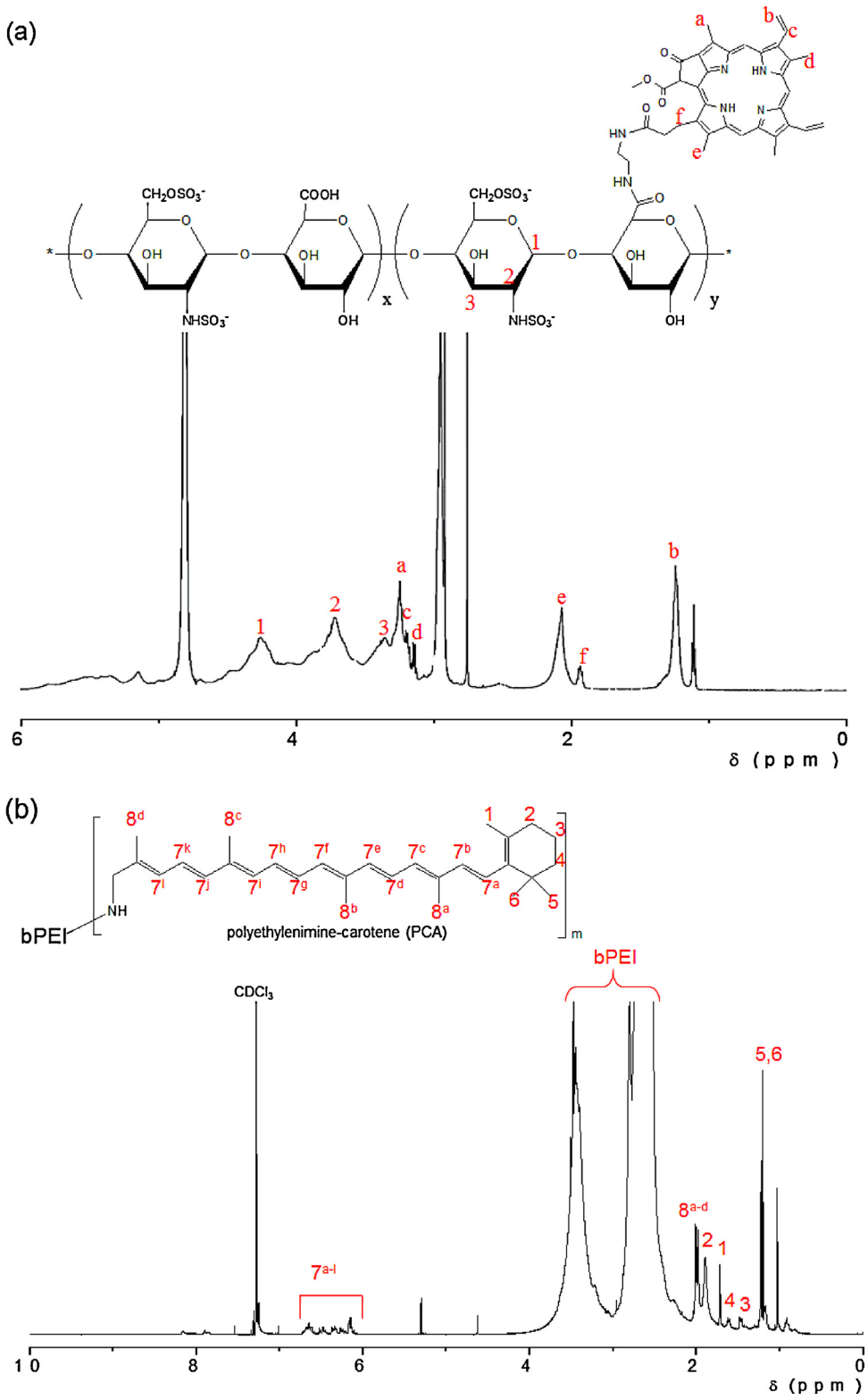

Fig. 3. ^{1}H NMR spectra of (a) the HPhA conjugate and (b) the PCAR conjugate.

hypothesized that PhA was efficiently solubilized in the HPhA/PCAR nanocomplex without severe aggregation or self-photoquenching.

3.3. Singlet oxygen scavenging and generation

To understand the scavenging effect of PCAR on singlet oxygen generated from HPhA in the nanocomplex, a DMA assay was performed in PBS to determine the SOQ. DMA is a fluorescent probe that can be converted to a non-fluorescent endoperoxide derivative via a selective reaction with singlet oxygen (Rapozzi et al., 2014). First, DMA control assays using HPhA/bPEI complex and HPhA conjugates were performed in PBS. Upon laser irradiation at 670 nm, the HPhA conjugates produced singlet oxygen; this was confirmed by observing the decrease in the fluorescence intensity of DMA

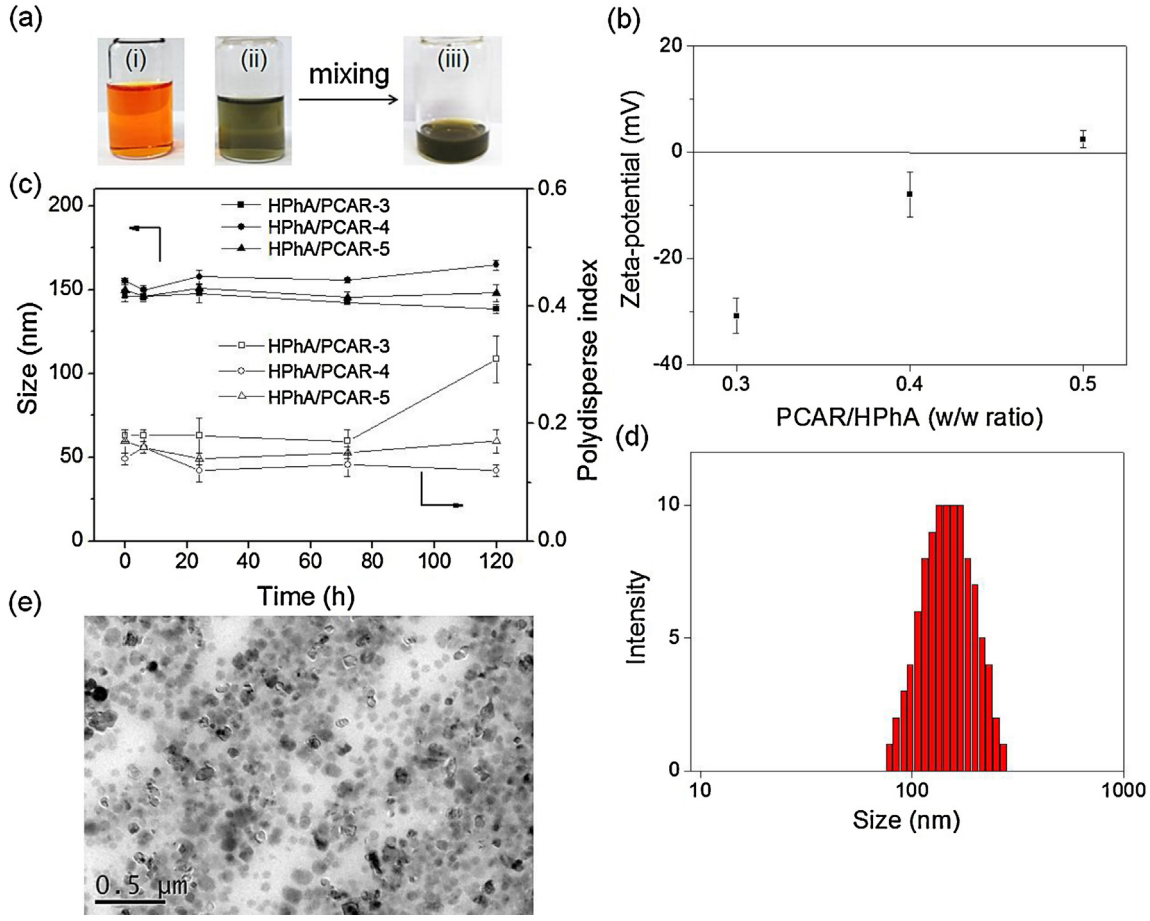

Fig. 4. Characterization of the HPhA/PCAR complex: (a) photographs representing water-soluble (i) PCAR, (ii) HPhA, and (iii) the HPhA/PCAR nanocomplex; (b) zeta-potential of HPhA/PCAR nanocomplexes with different PCAR/HPhA ratios; (c) stability test of HPhA/PCAR nanocomplexes in PBS; and representative (d) size distribution and (e) TEM image of the HPhA/PCAR nanocomplex.

over the irradiation time period (Fig. 6). The SOQ of the HPhA molecule was 0.41. The HPhA/PEI nanocomplex without PCAR also exhibited a sharp decline in DMA fluorescence intensity in PBS, demonstrating that rapid singlet oxygen generation occurred upon light exposure. The SOQ of the HPhA/PEI complex was calculated to be 0.40, similar to that of water-soluble HPhA conjugates. It was therefore confirmed that PhA-induced singlet oxygen generation was unaffected by the chemical conjugation of PhA to a water-soluble polymer and unaffected by the electrostatic complexation process.

No obvious decrease in the fluorescence intensity of DMA was observed for the HPhA/PCAR nanocomplex; the resulting SOQ was approximately 20-fold lower than those observed for HPhA conjugates and the HPhA/PEI complex. The suppressed release of singlet oxygen from the HPhA/PCAR nanocomplex could be attributed to low singlet oxygen production or to a PCAR-mediated scavenging

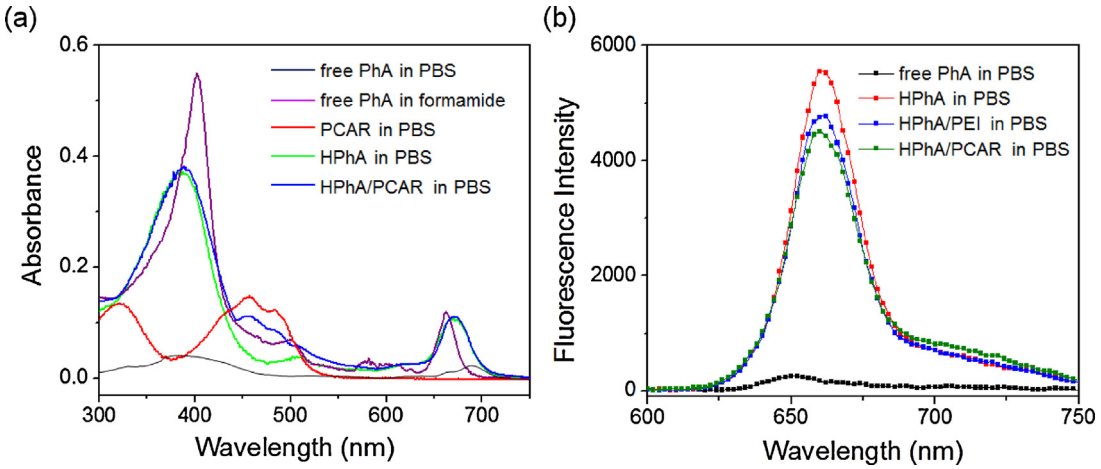

Fig. 5. (a) UV–vis spectra of free PhA, HPhA conjugates, PCAR conjugates, and the HPhA/PCAR nanocomplex in PBS and of free PhA in formamide; (b) fluorescence spectra of free PhA, HPhA conjugates, HPhA/PEI, and the HPhA/PCAR nanocomplex in PBS.

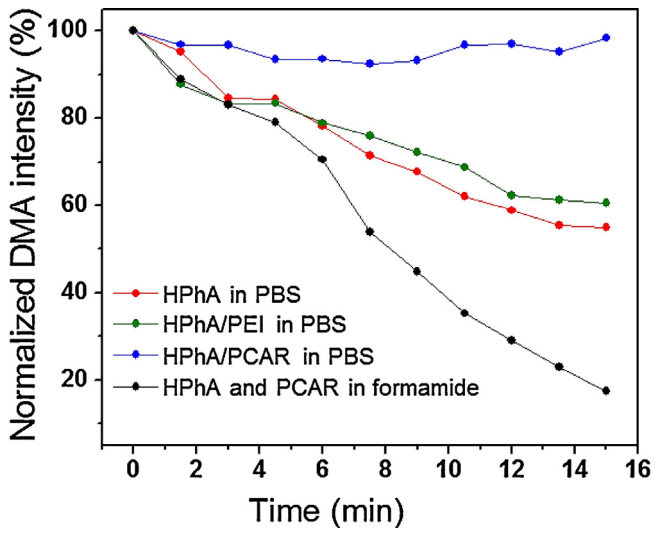

Fig. 6. Singlet oxygen generation by HPhA conjugates, HPhA/PEI, and the HPhA/PCAR nanocomplex in PBS and of HPhA and the PCAR mixture in formamide. The complex structure can become dissociated in chloroform, thereby restricting the co-existence of PhA and CAR; the HPhA/PCAR nanocomplex can retain its integrity in PBS.

effect. However, PhA molecules retained their singlet oxygen generation ability even after conjugation to a polymer. In addition, no measurable quenching effect was observed by the formation of a nanocomplex with PEI. Only the presence of CAR molecules in a nanocomplex can prevent the free diffusion of singlet oxygen. Thus, it can be concluded that the PhA molecules in the HPhA/PCAR complex generate singlet oxygen under light exposure. The singlet oxygen generated in this manner is then significantly scavenged by the CAR co-loaded in the complex. As a result, the nanocomplex of the polymeric photosensitizer HPhA can be used to improve the therapeutic efficacy of PDT. In particular, the polymeric scavenger PCAR can aid in the controlled release of singlet oxygen.

A promising activatable PS formulation should be non-toxic in the circulatory and extracellular compartments and efficiently produce singlet oxygen only at the target tissue and in malignant cells (Verhille et al., 2010). The fundamental mechanism of the solid-tumor targeting of the HPhA/PCAR nanocomplex is the EPR effect. As described earlier and shown in Fig. 6, the nanocomplex releases scant amounts of singlet oxygen as a stable nanoparticle structure in an aqueous environment. It is therefore expected that the HPhA/PCAR system would be non-toxic during circulation in the bloodstream and will be accumulated at the target tissue of a solid tumor. Nanoparticles can be internalized by endocytosis and/or pinocytosis (Zhao et al., 2011). It is well known that malignant cells exhibit high metabolic activity and high cellular movement (Brigger, Dubernet, & Couvreur, 2002). Therefore, the next and final destination of HPhA/PCAR nanoparticles should be intracellular compartments. To provide a successful activatable PS, nanocomplex systems must present their maximum therapeutic effect in an intracellular environment. It is generally accepted that nanoparticles, based on electrostatic complexation, can be dissociated into single molecules in the cytosol due to a relatively higher ionic strength, concentrated enzymes, various ionic species, and a lower pH (Cai, Ni, & Zhang, 2012; Luo, Wang, Yuan, & Gao, 2009).

To mimic the intracellular fate of the HPhA/PCAR nanocomplex, the nanocomplex was dissolved in the highly polar solvent formamide. Formamide dissolves both HPhA and PCAR molecules; therefore, PS and scavenger molecules can move away from each other, possibly beyond the effective Förster distance. Upon laser irradiation at 670 nm, the mixture of HPhA and PCAR in formamide efficiently produced singlet oxygen. The presence of singlet oxygen

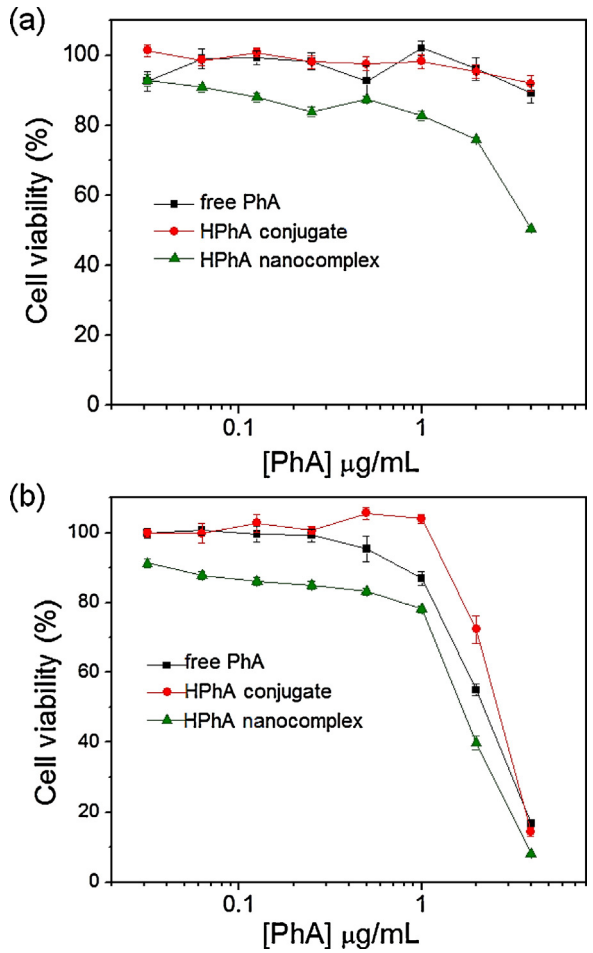

Fig. 7. (a) Dark toxicity and (b) phototoxicity of free PhA, HPhA conjugates, and the HPhA/PCAR nanocomplex toward MCF-7 cells.

was confirmed by the obvious decrease in the fluorescence intensity of DMA over time (Fig. 6). The resulting mixture of HPhA and PCAR conjugates in formamide appeared to have a slightly higher SOQ (0.47) than aqueous solutions of HPhA conjugates (0.41) or a HPhA/bPEI complex (0.40). This may be due to the longer half-life and travel distance of singlet oxygen in organic solvents. Fernandez et al. (1997) demonstrated that the singlet oxygen reaction was increased in solvents, trapping molecules and resulting in a sharp decline in the fluorescence of DMA. It should be noted that heparin takes advantage of enzymatic degradation in the lysosome, an intracellular organelle. Many glycosidases and several types of heparinases are located in the lysosome (Nilasaroya, Martens, & Whitelock, 2012). Therefore, the disintegration and degradation of the nanocomplex would be accelerated by enzyme activity; single-molecule changes may lead to the irreversible dissociation of PhA and CAR molecules. As a result, the HPhA/PCAR nanocomplex platform is a promising activatable PS system.

3.4. In vitro phototoxicity of the HPhA/PCAR nanocomplex in cancer cells

Dark toxicity and phototoxicity of the HPhA/PCAR nanocomplex was evaluated using MCF-7 cells. Toxicity results were compared with those for free PhA and the HPhA conjugate. In the tested concentration range, the free PhA molecules and the HPhA conjugate molecules exhibited little cell cytotoxicity. Cell viability under light-protected conditions was 90–102% and 92–101% for the free PhA and the HPhA-treated cells, respectively (Fig. 7(a)).

The HPhA/PCAR nanocomplex caused slight dark toxicity. This toxicity was likely caused by singlet oxygen generation, as discussed below.

The cytotoxicity of PCAR was also evaluated for MCF-7 cells. The results are presented as IC_{50} values (the drug concentration at which 50% growth inhibition occurs). The cytotoxicity of PCAR was 1.08 μg/mL in dark conditions and 1.09 μg/mL in light conditions (Fig. S2). We verified that free CAR is non-toxic for MCF-7 cells in a previous report (Li, Cho, et al., 2014). Therefore, the cytotoxicity of PCAR should be caused by the PEI moiety (e.g., 2 μg/mL of CAR equivalent contains c.a. 31 μg/mL bPEI). Because the HPhA did not demonstrate any obvious cytotoxicity in darkness, it could be concluded that the slight dark toxicity observed for HPhA/PCAR nanocomplex-treated cells was most likely due to the cytotoxic effect of the PEI in PCAR. PEI is a widely used cationic polymer in the biomedical field that exhibits some cytotoxicity (Lv, Zhang, Wang, Cui, & Yan, 2006). It has been reported that PEI is cytotoxic depending on its molecular weight and concentration (Godbey, Wu, & Mikos, 2001).

The PEI-induced cytotoxicity of HPhA/PCAR against MCF-7 cells, however, will not be a problem. This is because target cells should be killed by any means once the nanocomplex is delivered to the tumor site. The more pressing problem may be the net charge of the HPhA/PCAR nanocomplex. It is established that positively charged nanoparticles interact non-specifically with cells and proteins in the body (Verma & Stellacci, 2010). To minimize PEI-induced non-specific interactions, the net charge of a nanoparticle should be negative. In the current study, the weight ratio between PCAR and HPhA was 0.4; the zeta potential was slightly negative at −8.0. Whether this is an optimal condition for the maximum therapeutic efficacy of the HPhA/PCAR system should be examined using in vivo animal studies.

Following light treatment, the free PhA and the HPhA conjugate showed significant phototoxicity (IC_{50}; free PhA, 1.12 μg/mL; HPhA conjugates, 1.16 μg/mL). In addition, the HPhA/PCAR nanocomplex was also significantly phototoxic to MCF-7 cells (IC_{50} = 1.60 μg/mL, Fig. 7(b)). Because PCAR had a negligible effect on cytotoxicity independent of light treatment (Fig. S2), the enhanced cytotoxicity observed in the HPhA/PCAR-nanocomplex-treated cells after light treatment was most likely induced by the phototoxic effect of PhA. This result implies that the PhA in the nanocomplex effectively generated the cytotoxic species and induced cell death. Although the PhA-induced generation of singlet oxygen can be restricted due to CAR-mediated scavenging in an aqueous medium, the phototoxicity of the HPhA/PCAR nanocomplex in living cells was maintained; this was most likely due to spatial isolation between the HPhA and PCAR molecules in the intracellular environment. As described earlier, the enzymatic degradation of the heparin backbone or the dissociation/disintegration of the ionic complex structure could induce the deactivation of the scavenging effect.

Based on these findings, we propose the construction of a polyelectrolyte complex using oppositely charged polymeric PSs and scavengers to produce a reliable, activatable, and photosensitizing platform for selective PDT. The resulting polyelectrolyte complex nanoparticle exhibits controllable phototoxicity for photodynamic cancer therapy and is expected to modulate the pharmaceutical features and biodistribution of loaded PSs due to its nanoscale organization and appropriate surface properties. To the best of our knowledge, this is the first study to investigate the scavenging property of carotenoids that were physically formulated with PSs in a polyelectrolyte complex platform. The nanocomplexes formed by water-soluble HPhA and PCAR conjugates with opposite charges through an electrostatic interaction are also distinct from recently reported PhA/CAR dual-loaded polymeric micelles (Li, Cho, et al., 2014). In the previous report, the hydrophobic PhA and CAR molecules were directly formulated through a physical entrapment process. In this proof-of-principle study, our concept was verified using negatively charged heparin and positively charged bPEI as polyelectrolytes to formulate and solubilize the PS and scavenger. The results suggest that a similar complex nanocarrier platform could be fabricated using other ionic polymers (e.g., glycol chitosan, hyaluronic acid, polylysine, and polyglutamic acid) to achieve multi-functional photodynamic cancer treatments with greater safety.

4. Conclusion

We proposed a new strategy to develop a water-soluble PS with site-specific, controllable production of singlet oxygen. To construct an activatable PS, a polyelectrolyte nanocomplex was prepared via ionic interactions between oppositely charged HPhA and PCAR conjugates. The stable, nano-sized HPhA/PCAR nanocomplex can be obtained by adjusting the weight ratio of PCA to HPhA from 0.3 to 0.5. The spectrometric characteristics of the HPhA/PCAR nanocomplex demonstrated that the complex formation process and the co-existence of CAR did not induce the aggregation of PhA or photoquenching. The low release of singlet oxygen by the HPhA/PCAR nanocomplex upon light irradiation could only be explained by the scavenging activity of PCAR. In addition, we verified that spatial isolation between HPhA and PCAR invalidates the scavenging activity of PCAR. Such an effect can be expected in an intracellular environment; various biological components disintegrate complex structures and thus have a restrictive effect on scavenging activity. Additionally, we observed significant phototoxicity in cells treated with the HPhA/PCAR nanocomplex. These findings suggest that the HPhA/PCAR nanocomplex is a potential formulation that could provide controllable singlet oxygen generation for site-specific PDT.

Acknowledgment

This research was supported by the Basic Science Research Program through the National Research Foundation of Korea (NRF), funded by the Ministry of Education, Science and Technology (NRF-2012R1A1A2005029 and NRF-2013R1A2A2A04015914).

Appendix A. Supplementary data

Supplementary data associated with this article can be found, in the online version, at http://dx.doi.org/10.1016/j.carbpol.2014.12.035.

References

Brigger, I., Dubernet, C., & Couvreur, P. (2002). Nanoparticles in cancer therapy and diagnosis. *Advanced Drug Delivery Reviews*, *54*(5), 631–651.

Cai, H., Ni, C., & Zhang, L. (2012). Preparation of complex nano-particles based on alginic acid/poly[(2-dimethylamino) ethyl methacrylate] and a drug vehicle for doxorubicin release controlled by ionic strength. *European Journal of Pharmaceutical Sciences*, *45*(1–2), 43–49.

Chen, J., Jarvi, M., Lo, P. C., Stefflova, K., Wilson, B. C., & Zheng, G. (2007). Using the singlet oxygen scavenging property of carotenoid in photodynamic molecular beacons to minimize photodamage to non-targeted cells. *Photochemical and Photobiological Science*, *6*(12), 1311–1317.

Detty, M. R., Gibson, S. L., & Wagner, S. J. (2004). Current clinical and preclinical photosensitizers for use in photodynamic therapy. *Journal of Medicinal Chemistry*, *47*(16), 3897–3915.

Dolmans, D. E., Fukumura, D., & Jain, R. K. (2003). Photodynamic therapy for cancer. *Nature Reviews Cancer*, *3*(5), 380–387.

Eichwurzel, I., Stiel, H., & Roder, B. (2000). Photophysical studies of the pheophorbide a dimer. *Journal of Photochemistry and Photobiology B: Biology*, *54*(2–3), 194–200.

Fernandez, J. M., Bilgin, M. D., & Grossweiner, L. I. (1997). Singlet oxygen generation by photodynamic agents. *Journal of Photochemistry and Photobiology B: Biology*, *37*(1–2), 131–140.

Godbey, W. T., Wu, K. K., & Mikos, A. G. (2001). Poly(ethylenimine)-mediated gene delivery affects endothelial cell function and viability. *Biomaterials*, *22*(5), 471–480.

Hamblin, M. R., & Mróz, P. (2008). *Advances in photodynamic therapy: Basic, translational, and clinical*. Boston, MA: Artech House.
Juarranz, A., Jaen, P., Sanz-Rodriguez, F., Cuevas, J., & Gonzalez, S. (2008). Photodynamic therapy of cancer. Basic principles and applications. *Clinical and Translational Oncology*, *10*(3), 148–154.
Konan, Y. N., Gurny, R., & Allemann, E. (2002). State of the art in the delivery of photosensitizers for photodynamic therapy. *Journal of Photochemistry and Photobiology B: Biology*, *66*(2), 89–106.
Li, L., Bae, B. C., Tran, T. H., Yoon, K. H., Na, K., & Huh, K. M. (2011). Self-quenchable biofunctional nanoparticles of heparin-folate-photosensitizer conjugates for photodynamic therapy. *Carbohydrate Polymers*, *86*(2), 708–715.
Li, L., Cho, H., Yoon, K. H., Kang, H. C., & Huh, K. M. (2014). Antioxidant-photosensitizer dual-loaded polymeric micelles with controllable production of reactive oxygen species. *International Journal of Pharmaceutics*, *471*(1–2), 339–348.
Li, L., Nurunnabi, M., Nafiujjaman, M., Jeong, Y. Y., Lee, Y. K., & Huh, K. M. (2014). A photosensitizer-conjugated magnetic iron oxide/gold hybrid nanoparticle as an activatable platform for photodynamic cancer therapy. *Journal of Materials Chemistry B*, *2*(19), 2929–2937.
Li, L., Nurunnabi, M., Nafiujjaman, M., Lee, Y. K., & Huh, K. M. (2013). GSH-mediated photoactivity of pheophorbide a-conjugated heparin/gold nanoparticle for photodynamic therapy. *Journal of Controlled Release*, *171*(2), 241–250.
Linhardt, R. J. (1991). Heparin – An important drug enters its 7th decade. *Chemistry & Industry*, (2), 45.
Lovell, J. F., Chen, J., Jarvi, M. T., Cao, W. G., Allen, A. D., Liu, Y., et al. (2009). FRET quenching of photosensitizer singlet oxygen generation. *Journal of Physical Chemistry B*, *113*(10), 3203–3211.
Lovell, J. F., Liu, T. W. B., Chen, J., & Zheng, G. (2010). Activatable photosensitizers for imaging and therapy. *Chemical Reviews*, *110*(5), 2839–2857.
Luo, Y., Wang, A., Yuan, J., & Gao, Q. (2009). Preparation, characterization and drug release behavior of polyion complex micelles. *International Journal of Pharmaceutics*, *374*(1–2), 139–144.
Lv, H., Zhang, S., Wang, B., Cui, S., & Yan, J. (2006). Toxicity of cationic lipids and cationic polymers in gene delivery. *Journal of Controlled Release*, *114*(1), 100–109.
MacDonald, I. J., & Dougherty, T. J. (2001). Basic principles of photodynamic therapy. *Journal of Porphyrins and Phthalocyanines*, *5*(2), 105–129.
Maeda, H. (2001). The enhanced permeability and retention (EPR) effect in tumor vasculature: The key role of tumor-selective macromolecular drug targeting. *Advances in Enzyme Regulation*, *41*(1), 189–207.
Master, A., Livingston, M., & Sen Gupta, A. (2013). Photodynamic nanomedicine in the treatment of solid tumors: Perspectives and challenges. *Journal of Controlled Release*, *168*(1), 88–102.
McCarthy, J. R., & Weissleder, R. (2007). Model systems for fluorescence and singlet oxygen quenching by metalloporphyrins. *ChemMedChem*, *2*(3), 360–365.
Nehoff, H., Parayath, N. N., Domanovitch, L., Taurin, S., & Greish, K. (2014). Nanomedicine for drug targeting: Strategies beyond the enhanced permeability and retention effect. *International Journal of Nanomedicine*, *9*, 2539–2555.
Nilasaroya, A., Martens, P. J., & Whitelock, J. M. (2012). Enzymatic degradation of heparin-modified hydrogels and its effect on bioactivity. *Biomaterials*, *33*(22), 5534–5540.
Park, W., Park, S., & Na, K. (2011). The controlled photoactivity of nanoparticles derived from ionic interactions between a water soluble polymeric photosensitizer and polysaccharide quencher. *Biomaterials*, *32*(32), 8261–8270.
Rapozzi, V., Zorzet, S., Zacchigna, M., Della Pietra, E., Cogoi, S., & Xodo, L. E. (2014). Anticancer activity of cationic porphyrins in melanoma tumour-bearing mice and mechanistic in vitro studies. *Molecular Cancer*, *13*, 75.
Robert, B. (1986). Pheophorbide a – A new photosensitizer for PDT. *Studia Biophysica*, *144*, 183–186.
Verhille, M., Couleaud, P., Vanderesse, R., Brault, D., Barberi-Heyob, M., & Frochot, C. (2010). Modulation of photosensitization processes for an improved targeted photodynamic therapy. *Current Medicinal Chemistry*, *17*(32), 3925–3943.
Verma, A., & Stellacci, F. (2010). Effect of surface properties on nanoparticle–cell interactions. *Small*, *6*(1), 12–21.
Vrouenraets, M. B., Visser, G. W., Snow, G. B., & van Dongen, G. A. (2003). Basic principles, applications in oncology and improved selectivity of photodynamic therapy. *Anticancer Research*, *23*(1B), 505–522.
Wilson, B. C. (2002). Photodynamic therapy for cancer: Principles. *Canadian Journal of Gastroenterology*, *16*(6), 393–396.
Zhao, F., Zhao, Y., Liu, Y., Chang, X., Chen, C., & Zhao, Y. (2011). Cellular uptake, intracellular trafficking, and cytotoxicity of nanomaterials. *Small*, *7*(10), 1322–1337.